Bifunctional Tin Telluride Electrocatalysts for Oxygen Evolution and Reduction Reactions

Harish Singh[a], Amideddin Nouralishahi [a], Kurt Lagemann[a] and Manashi Nath[a]*

[a.] *Department of Chemistry, Missouri University of Science and Technology, Rolla, MO 65409, USA.*

Synthesis process:

For SnTe synthesis, Te powder (0.06 M) was dissolved in DI water, followed by the addition of NaOH and $SnCl_2 \cdot 2H_2O$ with stirring. $NaBH_4$ was then added, and the mixture was stirred for 45 minutes. The solution was transferred to a Teflon-lined autoclave and heated at 145 °C for 3 hours. The resulting black product was centrifuged, washed with DI water and ethanol, and vacuum-dried at 60 °C for 24 hours.

Electrode Preparation

To evaluate the OER and ORR activities of hydrothermally synthesized SnTe catalysts, a homogeneous catalyst ink was first prepared. This was achieved by dispersing 4 mg of catalyst in 300 µL of ethanol, followed by the addition of 0.8 µL of 5 wt% Nafion solution. For OER measurements, the ink was ultrasonicated for 1 hour to ensure uniform dispersion, and 100 µL of the resulting suspension was drop-cast onto a carbon cloth electrode (geometric area: 0.283 cm^2).

Prior to ORR measurements, the glassy carbon (GC) electrode (geometric area: 0.196 cm^2) was mechanically polished using 1.0 and 0.05 µm alumina slurry, followed by sequential sonication in isopropanol and deionized water to remove surface contaminants. Subsequently, 20 µL of the catalyst ink was drop-cast onto the GC electrode surface and allowed to dry under ambient conditions.

Materials Characterization :

X-ray Diffraction (XRD): The crystallographic structure of the SnTe electrocatalyst was examined using powder X-ray diffraction (PXRD). Diffraction patterns were obtained on a Philips X'Pert diffractometer equipped with a Cu Kα radiation source (λ = 1.5406 Å) and a Ni filter. Data were collected over a 2θ range of 5° to 80°, with a scanning rate of 0.05° s^{-1}, providing insight into phase purity and crystal structure.

Scanning Electron Microscopy (SEM) and Energy Dispersive X-ray Spectroscopy (EDS): The surface morphology of SnTe particles was analyzed using a FEI Helios Nanolab 600 SEM operated at an accelerating voltage of 10 kV and a working distance of 10 mm. Elemental composition and spatial distribution were further investigated via EDS mapping and point analysis using the same instrument.

X-ray Photoelectron Spectroscopy (XPS): The surface chemical states and elemental oxidation states of SnTe were characterized by X-ray photoelectron spectroscopy using a Thermo Scientific NEXSA surface analysis equipment. To obtain accurate surface information, all XPS measurements were performed on pristine (unsputtered) samples, ensuring that the native surface chemistry was preserved.

Electrochemical Characterization

The electrocatalytic activity of the synthesized materials toward the OER and ORR was evaluated using an IviumStat potentiostat in a standard three-electrode electrochemical setup. A graphite rod served as the counter electrode, and a saturated Ag|AgCl electrode was used as the reference.

For ORR measurements, a 5 mm rotating ring-disk electrode (RRDE) was employed as the working electrode, while for OER studies, catalyst-coated carbon cloth was used. OER testing was conducted in N_2-saturated 1 M KOH, whereas ORR measurements were performed in O_2-saturated 1 M KOH at various electrode rotation speeds ranging from 400 to 2000 rpm, with a scan rate of 10 mV s^{-1}. To determine the electron transfer number (n) involved in the ORR process, Koutecky–Levich (K–L) analysis was performed. The K–L plots (J^{-1} vs. $\omega^{-1/2}$) were constructed at different potentials between 0.2 V and 0.8 V and fitted using the K–L equation (Eq. 1):

$$1/J = 1/J_L + 1/J_K = 1/B\omega^{1/2} + 1/J_K \qquad \text{Eq-1}$$

where **J** is the measured current density (mA cm^{-2}), **J_K** and **J_L** are the kinetic and diffusion-limited current densities, respectively, and **ω** is the electrode rotation rate (rpm). The slope (**B**) is defined by the Levich equation (Eq. 2):

$$B = 0.62nFC_0 (D_0)^{2/3}\upsilon^{-1/6} \qquad \text{Eq-2}$$

Here, **F** is the Faraday constant (96,485 C mol^{-1}), **n** is the number of electrons transferred per O_2 molecule, $\mathbf{C_0}$ is the bulk concentration of O_2 (1.2×10^{-6} mol cm^{-3}), $\mathbf{D_0}$ is the diffusion coefficient of O_2 (1.9×10^{-5} cm^2 s^{-1}), and **v** is the kinematic viscosity of the electrolyte (0.01 cm^2 s^{-1}). This analysis provides insight into the ORR pathway and the catalytic efficiency of the material.

Electrodeposition of Pt and RuO_2

Platinum was electrodeposited using a two-step potential method from an electrolyte containing 5 mM K_2PtCl_6 and 0.5 M H_2SO_4. The deposition was carried out by applying a potential step from 0.8 V to –0.25 V for 5 seconds, followed immediately by a step from –0.25 V to 0.25 V for 25 seconds.

For RuO_2 deposition, a glassy carbon (GC) substrate was used. The precursor solution was prepared by dissolving 0.452 g of $RuCl_3$ and 2.952 g of KCl in 40 mL of 0.01 M HCl. Electrodeposition was performed via cyclic voltammetry over a potential window of 0.015 to 0.915 V (vs. Ag|AgCl) for 100 cycles at a scan rate

of 50 mV s^{-1}. The resulting film was then annealed in air at 200 °C for 3 hours to achieve crystallization and oxidation to RuO_2.

Table S1: Comparative Electrocatalytic Activity of SnTe and Other Reported Sn-Based and State of art RuO_2 catalysts for OER.

OER Catalyst	Electrolyte (pH)	η @ 10 mA·cm^{-2} (mV vs RHE)	Tafel slope (mV·dec^{-1})	Reference
SnTe	1M KOH (alkaline)	340	103.7	This Work
SnTe	1M PBS (Neutral)	365	146.9	This Work
RuO_2	1M KOH (alkaline)	380	114.9	This Work
SnO_2/MnTe	1.0 M KOH (alkaline)	181	33	1
SnO_2/MnO_2	1.0 M KOH (alkaline)	360	38.9	2
CdSe/SnO_2	1.0 M KOH (alkaline)	233	89	3
$SnSe_2$	1.0 M KOH (alkaline)	375	322	4
SnS_2	1.0 M KOH (alkaline)	420	150	5
SnS_2	1M PBS (Neutral)	1450	177	5
SnO_2-Co_3O_4-Mo_2S_3	2.0 M KOH (alkaline)	192	~99	6
SnS-Sn_2S_3	1.0 M KOH (alkaline)	359	90.1	7
NiO–SnO_2	1.0 M KOH (alkaline)	600	—	8
NiFe-LDH-Sn/ZIF-67	---	360	79	9
Co-doped SnS2	1.0 M KOH (alkaline)	323	—	10
RuO_2	1M KOH (alkaline)	480	133	11

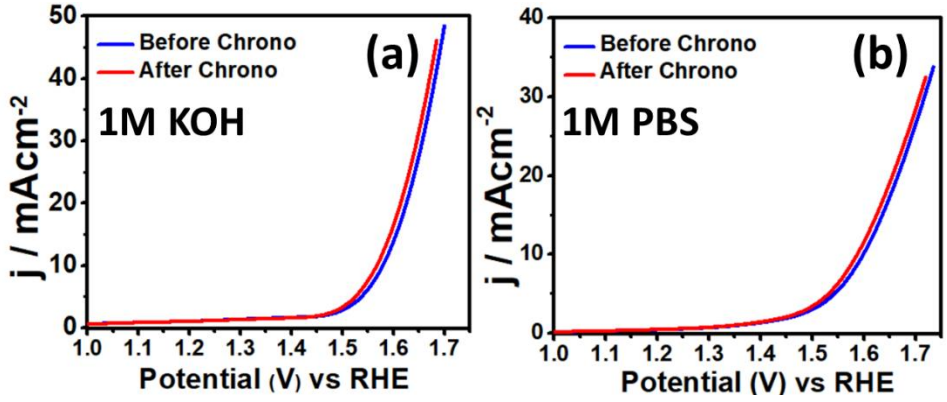

Figure S1. LSV before and after chronoamperometry in (a) 1 M KOH and (b) 1 M PBS solution.

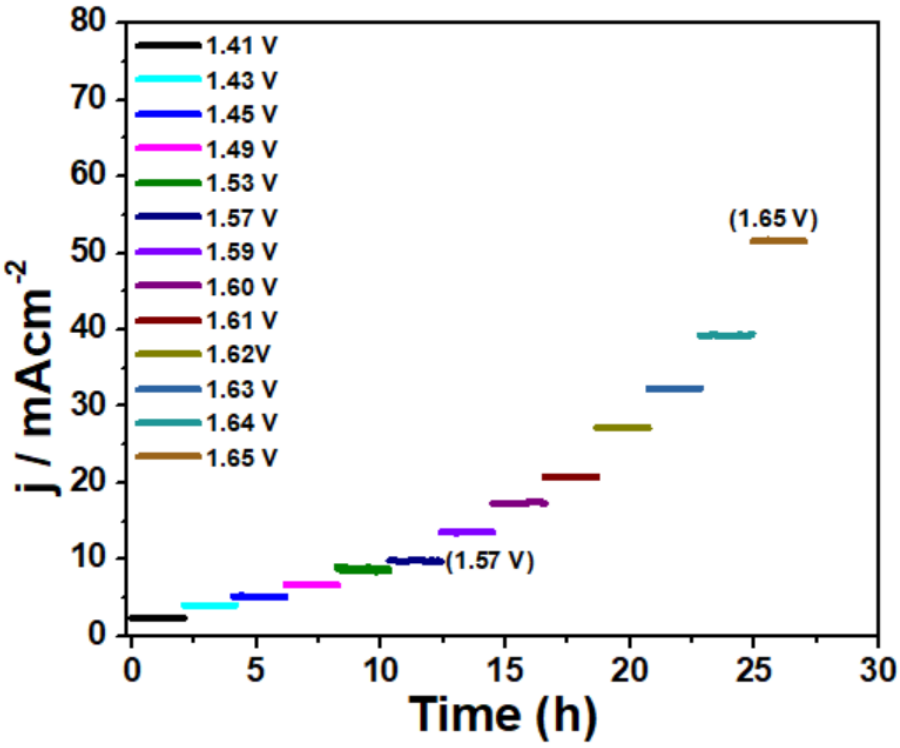

Figure S2. Multistep chronoamperometry test of the SnTe electrode carried out at various constant applied potentials.

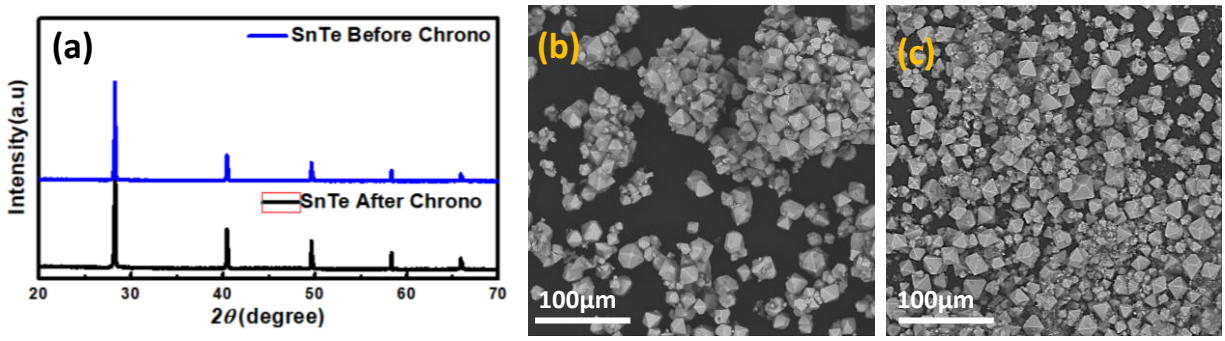

Figure S3. (a) XRD of SnTe before and after chronoamperometry. SEM of SnTe octahedral microcrystals (b) before chronoamperometry, and (c) after chronoamperometry.

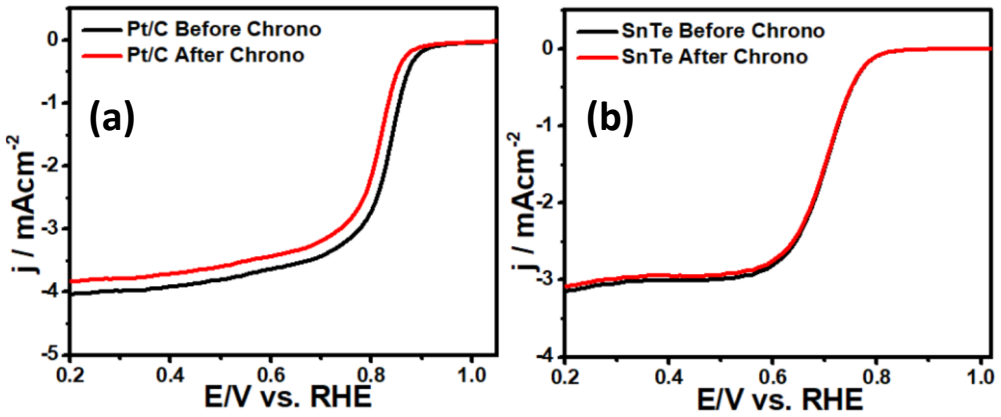

Figure S4. LSV plots of (a) Pt/C catalyst and (b) SnTe catalyst before and after chronoamperometry.

References

1 R. Zahra, A. W. Alrowaily, B. M. Alotaibi, H. A. Alyousef, N. Al-Harbi, A. Dahshan, K. Ahmad and A. M. A. Henaish, *J. Alloys Compd.*, 2024, **1000**, 175036.

2 N. Alwadai, S. Manzoor, M. Al Huwayz, M. Abdullah, R. Y. Khosa, S. Aman, A. G. Abid, Z. A. Alrowaili, M. S. Al-Buriahi and H. M. T. Farid, *Surfaces and Interfaces*, 2023, **36**, 102467.

3 M. U. Nisa, S. Manzoor, A. G. Abid, N. Tamam, M. Abdullah, M. Najam-Ul-Haq, M. S. Al-Buriahi, Z. A. Alrowaili, Z. M. M. Mahmoud and M. N. Ashiq, *Fuel*, 2022, **321**, 124086.

4 R. Fatima, K. Yusuf, M. S. Khan and M. U. Nisa, *Electrochim. Acta*, 2024, **508**, 145279.

5 I. Fareed, · Masood, H. Farooq, · Muhammad, D. Khan, F. Khan, M. Firdous, Z. Asghar, Y. Sandali, · Muhammad Tahir, · Faheem, K. Butt and F. K. Butt, *Carbon Lett. 2025*, 2025, 1–14.

6 P. P. K. Sharma, P. Chaubey and S. Sarkar, , DOI:10.2139/SSRN.5109990.

7 R. Kumar Mishra, G. Jin Choi, R. Verma, S. Hun Jin, R. Bhardwaj, S. Arya, J. Singh and J. Seog Gwag, *Mater. Sci. Eng. B*, 2024, **303**, 117292.

8 M. Wu, Y. Li, J. Du, C. Tao and Z. Liu, *ACS Omega*, 2020, **5**, 22652.

9 R. Ahmed, A. E. Allah, A. A. Farghali, W. M. A. El Rouby and A. Abdelwahab, *Nanoscale Adv.*, 2025, **7**, 5401–5410.

10 J. H. Park, J. C. Ro and S. J. Suh, *Curr. Appl. Phys.*, 2022, **42**, 50–59.

11 Y. Zhang, Y. Wang, W. Sun, D. Ma, J. Ma, J. Rao, Q. Xu, J. Huo, J. Liu and G. Li, *Adv. Mater. Interfaces*, 2023, **10**, 2300279.